Investigations of the Viscoelastic Properties of Thin Polymer Films by Electromechanical Interferometry

H.-J. Winkelhahn, T. Pakula, and D. Neher*

MPI für Polymerforschung, Ackermannweg 10, D-55128 Mainz, Germany

Received January 19, 1996; Revised Manuscript Received July 18, 1996[⊗]

ABSTRACT: A new experimental technique which allows determination of viscoelastic properties of thin polymer films with thickness of the order of micrometers and below is presented. The method consists of sandwiching the polymer film between two metal electrodes and detecting the periodic deformation due to an alternating electric field applied between the electrodes. A Nomarski optical interferometer was used to record the thickness changes of the order of nanometers. Exemplary results are presented for a 2.1 μm thick film of poly(methyl methacrylate). Both temperature and frequency dependencies have been determined. The analysis of the electromechanical data yielded both the real and imaginary parts of the compressibility of the thin film. The softening of the polymer around the glass transition temperature could be clearly resolved. The comparison to the bulk moduli yielded the temperature dependence of Poisson's ratio. Relaxation times deduced from electromechanical experiments at temperatures from 30 to 150 °C and frequencies between 80 Hz and 32 kHz agreed well with those determined by bulk mechanical and dielectric spectroscopy.

Introduction

Organic thin films are of potential interest with respect to various applications such as coatings, paints, resists, or even waveguides and light emitting devices. The properties of such films are generally correlated to the morphology of the organic film, characterized for example by the molecular order, macroscopic orientation, or degree of crystallization. Dynamic mechanical spectroscopy is known to be a strong and sensitive tool to probe many of these parameters. It is thus desirable to investigate in situ the mechanical properties of thin organic films.

Various methods such as surface force,[1] quartz crystal resonator,[2] nanoindendation,[3] Brillouin scattering,[4] and a beam bending technique[5] have been employed to obtain quantitative values of the mechanical moduli of thin films with thickness down to the nanometer thickness range. However, these methods have no or only limited tunability with respect to frequency. The determination of relaxation times or the construction of so-called master curves is thus difficult or even impossible. We have recently demonstrated that absolute values of the compressibility of thin polymeric films can be determined by measuring the electric field induced change in film thickness with optical interferometry.[6] This change is caused by two contributions, that is the Maxwell stress applied by the oppositely charged electrodes and by electrostriction due to changes in the dielectric constant during film deformation. In this paper, we report on the determination of mechanical properties as a function of temperature and frequency. The electric field induced compression is shown to be a direct way to address the dynamic compressibility and E modulus of a PMMA film with thickness in the micrometer range. The results are compared to data from dielectric spectroscopy and bulk mechanical properties.

Theory

As outlined in the Experimental Section, the sample consists of a thin organic film sandwiched between two metal electrodes separated by a distance h. The organic layer itself is characterized by its complex dielectric function:

$$\epsilon(\omega) = \epsilon'(\omega) - i\epsilon''(\omega) \tag{1}$$

The electric behavior of the layer can thus be represented as a parallel connection of a resistor R and capacity C, whose values are given by[7]

$$R(\omega) = \frac{1}{\omega\epsilon''(\omega)C_0} \tag{2a}$$

$$C(\omega) = \epsilon'(\omega)C_0 \tag{2b}$$

$$C_0 = \epsilon_0\frac{A}{h} \tag{2c}$$

C_0 is the value for the unfilled capacitor of area A separated by a distance h. Upon application of an external voltage U across the sample, both the resistive and capacitive parts will contribute independently to a change in film thickness.

In order to evaluate the size of the capacitive contribution, we consider a capacitor with electrode area A at a distance h. The space between the electrode is in part filled with a dielectric medium of thickness $d \le h$ and dielectric constant ϵ'. The energy of the capacitor loaded with a total charge Q is then

$$W = \frac{Q^2}{2\epsilon_0 A}[h - d + d/\epsilon'] \tag{3}$$

In this case, the force between the electrodes (Maxwell force) is given by

$$F_{\mathrm{M}} = -\frac{\partial W}{\partial h} = -\frac{Q^2}{2\epsilon_0 A} \tag{4a}$$

and the force on the dielectric medium (electrostriction) by

$$F_{\mathrm{E}} = -\frac{\partial W}{\partial d} = \frac{Q^2}{2\epsilon_0 A}\left[1 - \frac{1}{\epsilon'} - \frac{(\epsilon'+2)(\epsilon'-1)}{3(\epsilon')^2}\right] \tag{4b}$$

* To whom correspondence should be addressed.

[⊗] Abstract published in *Advance ACS Abstracts,* September 1, 1996.

S0024-9297(96)00080-0 CCC: $12.00

The Claussius−Musotti equation has been used in the derivation of eq 4b:

$$\frac{\partial \epsilon'}{\partial d} = -\frac{(\epsilon' + 2)(\epsilon' - 1)}{3d} \tag{5}$$

The Maxwell force is always compressive while the electrostrictive force will lead to an expansion or a compression of the dielectric medium depending on the value of ϵ'.

In our geometry, the capacitor is completely filled ($d = h$) and the electrodes are directly fixed to the film ($\Delta d = \Delta h$). The total force is thus the sum of the two contributions, yielding a total attractive force between the plates of the capacitor:

$$F = F_{\mathrm{M}} + F_{\mathrm{E}} = -\frac{Q^2}{2\epsilon_0 \epsilon' A}\left[1 + \frac{(\epsilon' + 2)(\epsilon' - 1)}{3\epsilon'}\right] \tag{6a}$$

It can easily be shown that the same force results for the case of a constant applied voltage, where additional charges are supplied by an external voltage source.[8] Thus by replacing Q by $U \times C$ and using eq 2, the total force can be rewritten as

$$F = -\frac{\epsilon_0 A U^2}{2h^2}\left[\epsilon' + \frac{(\epsilon' + 2)(\epsilon' - 1)}{3}\right] \tag{6b}$$

This force causes a compression of the film:

$$\frac{\Delta h}{h} = \kappa_{\mathrm{p}} \frac{F}{A} \tag{7}$$

κ_{p} is an effective plate compressibility which will be further discussed below. The resulting change in thickness induced by the electric field is

$$\frac{\Delta h}{h} = -\frac{\epsilon_0 \kappa_{\mathrm{p}}}{2}\left[\epsilon' + \frac{(\epsilon' + 2)(\epsilon' - 1)}{3}\right]\frac{U^2}{h^2} \tag{8}$$

For a sinusoidal voltage with amplitude U_0 and frequency ω, both contributions will cause a periodic change in the film thickness but with twice the driving frequency:

$$\frac{\Delta h}{h}(2\omega) = -\frac{\epsilon_0 \kappa_{\mathrm{p}}(2\omega)}{2}\left[\epsilon'(\omega) + \frac{(\epsilon'(\omega) + 2)(\epsilon'(\omega) - 1)}{3}\right]\frac{{U_0}^2}{2h^2}\cos(2\omega t) \tag{9}$$

In the following, the frequencies of the applied electric field and of the thickness modulation will be called "driving frequency" (corresponding to ω) and "modulation frequency" (corresponding to 2ω), respectively.

The resistive contribution characterized by R ($\epsilon'' \neq 0$) leads to an energy dissipation W_{R} in the sample, which for a half period of the sinusoidal driving voltage is

$$W_R = \frac{{U_0}^2}{2R}\frac{\pi}{\omega} \tag{10}$$

As a result, the temperature of the sample will increase by

$$\Delta T = \frac{W_R}{c_p \rho V} \tag{11}$$

(V is the volume, ρ is the density, and c_p is the heat capacity of the sample at constant pressure) and, through the linear thermal expansion characterized by the linear thermal expansion coefficient α, the film expands:

$$\frac{\Delta h}{h} = \alpha \Delta T \tag{12}$$

Combining eqs 10−12 yields the change in film thickness due to the heat dissipated in the film:

$$\frac{\Delta h}{h} = \frac{\alpha \pi \epsilon_0 \epsilon''}{2\rho c_p}\frac{{U_0}^2}{h^2} \tag{13}$$

A periodic change in film thickness with the maximum amplitude given by eq 13 will occur only if the frequency of the applied sinusoidal voltage corresponds approximately to the time the sample needs to relax after a temperature step (adiabatic case). For frequencies lower than that, the temperature of the film will remain the same as the substrate temperature; for higher frequencies a steady-state temperature rise will be established.

Both the resistive contribution (eq 8) and the capacitive contribution (eq 13) have the same $(U_0/h)^2$ dependence but inverse sign.

$$\frac{\Delta h}{h}(2\omega) = \left\{\frac{\alpha \pi \epsilon_0 \epsilon''(\omega)}{2\rho c_p} - \frac{\epsilon_0 \kappa_{\mathrm{p}}(2\omega)}{2}\left[\epsilon'(\omega) + \frac{(\epsilon'(\omega) + 2)(\epsilon'(\omega) - 1)}{3}\right]\right\}\frac{{U_0}^2}{2h^2}\cos(2\omega t) \tag{14}$$

To obtain a rough estimate of the electric field induced change in film thickness due to the capacitive contribution, we have assumed a film thickness $h = 1\ \mu$m, an applied voltage $U = 100$ V, a real part of the dielectric constant $\epsilon' = 3.0$, and a compressibility of 2×10^{-10} Pa^{-1} as being typical for many (nonconjugated) polymers in the glassy state.[9] With eq 14 this gives a capacitive contribution $\Delta h \approx 30$ pm. As we will discuss later, this contribution should dominate the change in film thickness induced by the electric field for most polymeric systems.

The particular sample geometry as described in the Experimental Section implies that the film is fixed in the plane onto the substrate and that the thickness h of the film is about a factor of 1000 smaller than the lateral extension. For an infinitely stiff substrate, an expansion in the film plane upon vertical compression is thus not possible. To evaluate the effective compressibility of a film in this geometry, we consider the following equations which describe the strain e as a function of an applied stress σ

$$e_{11} = \frac{1}{E}[\sigma_{11} - \nu(\sigma_{22} + \sigma_{33})] \tag{15a}$$

$$e_{22} = \frac{1}{E}[\sigma_{22} - \nu(\sigma_{11} + \sigma_{33})] \tag{15b}$$

$$e_{33} = \frac{1}{E}[\sigma_{33} - \nu(\sigma_{11} + \sigma_{22})] \tag{15c}$$

Here, E is the Young's modulus, which is assumed to be isotropic and ν is Poisson's ratio. Since the film is

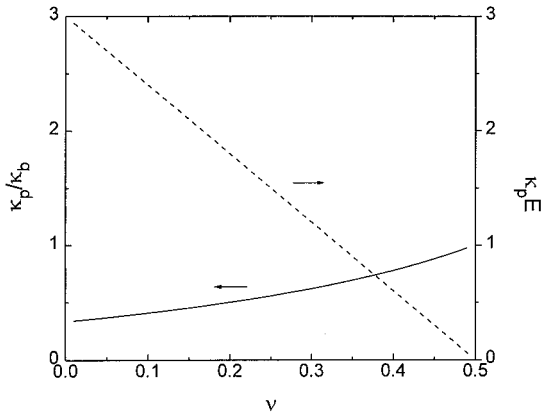

Figure 1. Ratio of the effective plate compressibility κ_p and the dynamic bulk compressibility κ_b (solid line) and κ_p times the Young's modulus E (dotted line) as a function of Poisson's ratio ν. The graphs are calculations based on eqs 17 and 18.

clamped to the substrate, the in-plane strain coefficients e_{11} and e_{22} are equal to zero and $e_{33} = \Delta h/h$. Solving the coupled eqs 15a−c yields

$$\frac{\Delta h}{h} = \kappa_p \sigma_{33} = \frac{\sigma_{33}}{E}\left(1 - \frac{2\nu^2}{1-\nu}\right) \tag{16}$$

The Young's modulus is further related to the dynamic bulk compressibility κ_b by[9]

$$\kappa_b = \frac{3}{E}(1 - 2\nu) \tag{17}$$

We finally obtain a relation between the effective plate compressibility κ_p and κ_b:

$$\kappa_p = \frac{(1 - 2\nu^2)/(1 + \nu)}{3(1 - 2\nu)}\kappa_b \tag{18}$$

κ_p is not only a function of κ_b or E but also depends on Poisson's ratio ν. In Figure 1 κ_p/κ_b and $\kappa_p E$ are plotted as a function of ν. Note that for a given E and $\nu = 0.5$, the material becomes incompressible. As a consequence $\kappa_p E$ varies strongly over the considered range of ν between 0 and 0.5. However, the ratio κ_p/κ_b changes only slightly. The result of the electromechanical experiment in the given geometry is thus more correlated to the bulk compressibility rather than to Young's modulus.

Experimental Section

Conventional poly(methyl methacrylate) (PMMA) was purchased from Aldrich with a molecular weight $M_w = 101\,000$. The 2.1 μm thick PMMA film was prepared by spin-coating from solution.

The experimental setup for the electromechanical measurements, which is a modified version of the interferometer published originally,[6] is shown in Figure 2.

The sample consists of a thin film sandwiched between a larger bottom electrode and two reflecting top electrodes. At these electrodes two orthogonal polarized beams (after passing a calcite prism) are reflected. When an electric field is applied between only one of the top electrodes and the bottom electrode, a phase shift ϕ is generated between the two beams, which is related to the field-induced change in film thickness by

$$\phi = \frac{4\pi}{\lambda}\Delta h \tag{19}$$

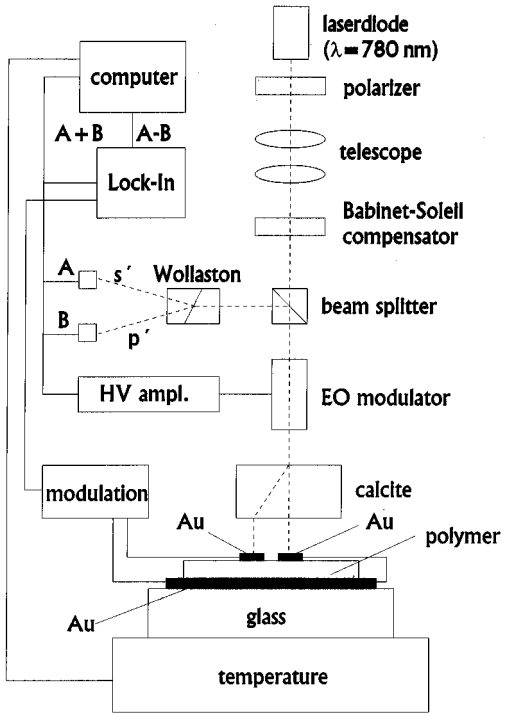

Figure 2. Experimental setup of the optical Nomarski interferometer and sample geometry.

After reflection the two beams are recombined in the calcite prism. In the detection arm of the interferometer the beam is split by a Wollaston prism into two beams with intensities A and B of orthogonal polarization and directed onto two photodiodes. When the optical axis of the Wollaston prism is rotated by 45° with respect to the optical axis of the calcite prism, the difference of the intensities A and B becomes proportional to the phase shift ϕ. At the working point of the interferometer, $A \approx B$, the difference of the two diode signals is proportional to the change in film thickness:

$$\frac{A - B}{A + B} = V \sin(\phi) \cong V\frac{4\pi}{\lambda}\Delta h \tag{20}$$

V is a contrast factor which is determined in a separate experiment. An electrooptical modulator (Gsaenger) is used to stabilize the working point of the interferometer as well as to determine the contrast factor V. In the experiment, the sinusoidal voltage is supplied by a Kontron function generator combined with a voltage amplifier. The modulation in the diode intensities A and B and thus in phase shift ϕ is analyzed directly by as lock-in amplifier (EG&G).[6] Absolute diode signals were recorded via an AD converter.

The chosen sample geometry has a particular advantage compared to the original setup, where one of the two probe beams had been reflected on a separate mirror. It has been recognized that the periodic compression of the film can induce strong bending modes of the underlying substrate at distinct modulation frequencies, which severely disturb the experiment.[10] In the improved version of the interferometer, both beams are reflected at the same substrate, reducing the effect of substrate vibrations. In addition, the substrate, typically of 1 mm thickness, is glued onto a second glass plate of slightly larger thickness. Only after these precautions the vibrational modes could be sufficiently suppressed.

The viscoelastic properties of bulk PMMA have been determined under shear deformation using a Rheometics RMS 800 mechanical spectrometer. Different sample geometries have been used: rectangular bars of dimensions 48 × 10 × 1.2 mm and a plate−plate geometry (with a plate diameter of 6 mm and a distance between the plates of 1.2 mm) for measurements below and above the glass transition, respectively. Results at various frequencies have been obtained simultaneously using the so-called multiple frequency sweep technique

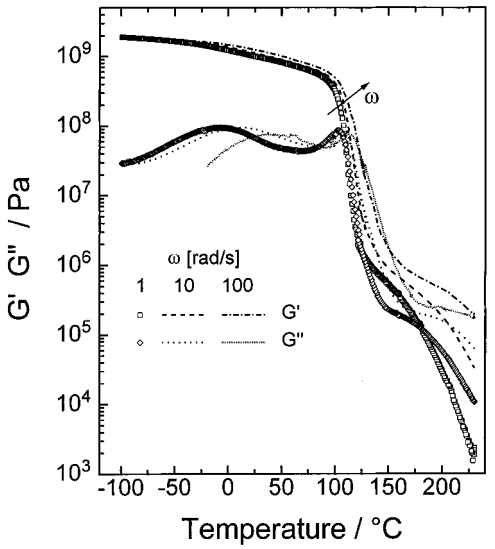

Figure 3. Temperature dependence of the real and imaginary parts of the bulk shear modulus (G' and G'') of PMMA for three different modulation frequencies.

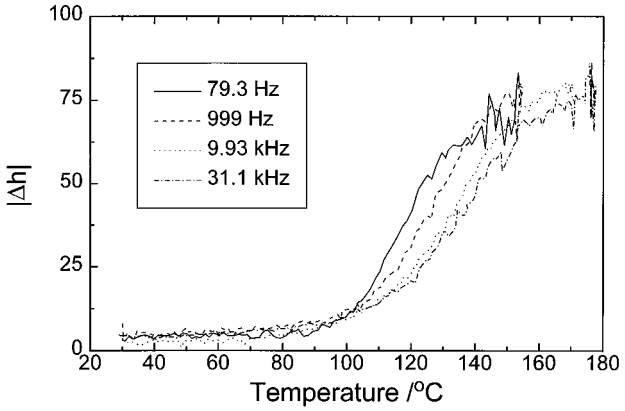

Figure 4. Absolute value of the electric field induced change in film thickness Δh as a function of temperature for four different modulation frequencies. A sinusoidal driving voltage $U_0 = 100$ V was applied to one of the two top electrodes. The thickness of the PMMA film was 2.1 μm.

and are shown in Figure 3. Independent frequency sweeps at various temperatures above T_g have been used for the construction of a master curve and to determine frequency shift factors log a_T as a function of temperature with respect to a reference temperature.

Dielectric spectroscopy was performed using a commercial Solatron-Schlumberger SI 1260 analyzer on melt-pressed samples of 50 μm thickness between two gold-covered brass plates.

Results and Discussion

Figure 4 shows the absolute value of the electric field induced change in film thickness as a function of temperature for a 2.1 μm thick PMMA film, measured at four different modulation frequencies (2ω). In all cases, the modulation voltage was 100 V. One observes a clear softening of the film at a temperature close to the glass transition ($T_g = 105$ °C), which shifts to higher temperature with increasing modulation frequency. This indicates viscoelastic behavior as typically observed for glass-forming polymers.

Dielectric spectra measured on the same material are shown in Figure 5. The frequency dependence of ϵ'' as a function of frequency is dominated by a conductivity contribution in the low-frequency region and the β-relaxation process assigned to the rotation of the $COOCH_3$ side group. As reported by others, the α-relaxation can be barely or not at all resolved in the dielectric spectra.[11]

The plate compressibility κ_p was determined from the electromechanical data using the equations derived in the theoretical section in combination with the experimental values for ϵ' and ϵ''. For example, Figure 6 shows the temperature dependence of the real and imaginary parts of the plate compressibility κ_p as determined from the electromechanical experiment for a modulation frequency of 993 Hz. The softening in the real part of κ_p corresponds to a clear loss peak in the imaginary part. Values for κ_p' at room temperature are approximately 0.1 GPa^{-1}, which is smaller than the dynamic bulk compressibilities, ranging between 0.2 and 0.25 GPa^{-1} for PMMA given in refs 9, 12, and 13. Note that $\kappa_p = \kappa_b$ only for a Poisson's ratio of 0.5. Above T_g, $\kappa_p \cong 0.7$ GPa^{-1}, which agrees well with values of κ_b between 0.5 and 0.65 GPa^{-1} of PMMA.[12,13] A direct determination of the Young's modulus from the electrostriction data is quite inaccurate without knowledge of Poissons ratio. Assuming $\nu = 0.33$, values for E' range between 7.5 and 10 GPa at room temperature, with a slight tendency to increase at higher modulation frequencies. Both Koppelmann et al.[14] and Yee et al.[15] consistently found storage moduli increasing from 3.3 GPa at 10 mHz, 3.8 GPa at 1 Hz, to approximately 5.2 GPa at 10 kHz. The discrepancy with our data underlines the difficulty in determining E from the electromechanical data without knowledge of Poisson's ratio.

The temperature dependence of ν could be derived via a direct correlation of the experimental shear modulus G' with the electromechanical compressibility κ_p' as shown in Figure 7. Combining the relation

$$G = \frac{E}{2(1+\nu)} \tag{21}$$

and eqs 8, 9, and 16 yields

$$\nu = -\frac{p}{2} + [(p^2/4 + q^2)]^{1/2} \tag{22a}$$

with

$$p = \frac{1}{2(1-\kappa_p G)} \tag{22b}$$

$$q = \frac{1-2\kappa_p G}{2(1-\kappa_p G)} \tag{22c}$$

Figure 7 depicts the temperature dependence of ν using the shear modulus measurement at $\omega = 100$ Hz and the electromechanical compressibility at $\omega = 6.2$ kHz, which showed the lowest scattering over the whole temperature range. Below T_g Poisson's ratio ν varies between 0.43 and 0.45, which is slightly larger than the literature values, ranging between 0.3 and 0.42.[14,15] The discrepancy might be in part due to the difference in modulation frequencies in the shear and electromechanical experiment. Above T_g, ν shows a steep increase up to 0.5. Schenkel has published the temperature dependence of ν for PMMA between 20 and 140 °C.[14] He observed a slight continuous increase from 0.32 at 20 °C, 0.42 at 100 °C, to 0.5 above 130 °C. In agreement with this, Yee reported ν ranging from 0.34 at −40 °C to 0.43 at 100 °C.[15] The rough correspondence of our data to these findings clearly supports our assumption that the film is fixed to the substrate and that lateral expanding can not occur in the sample

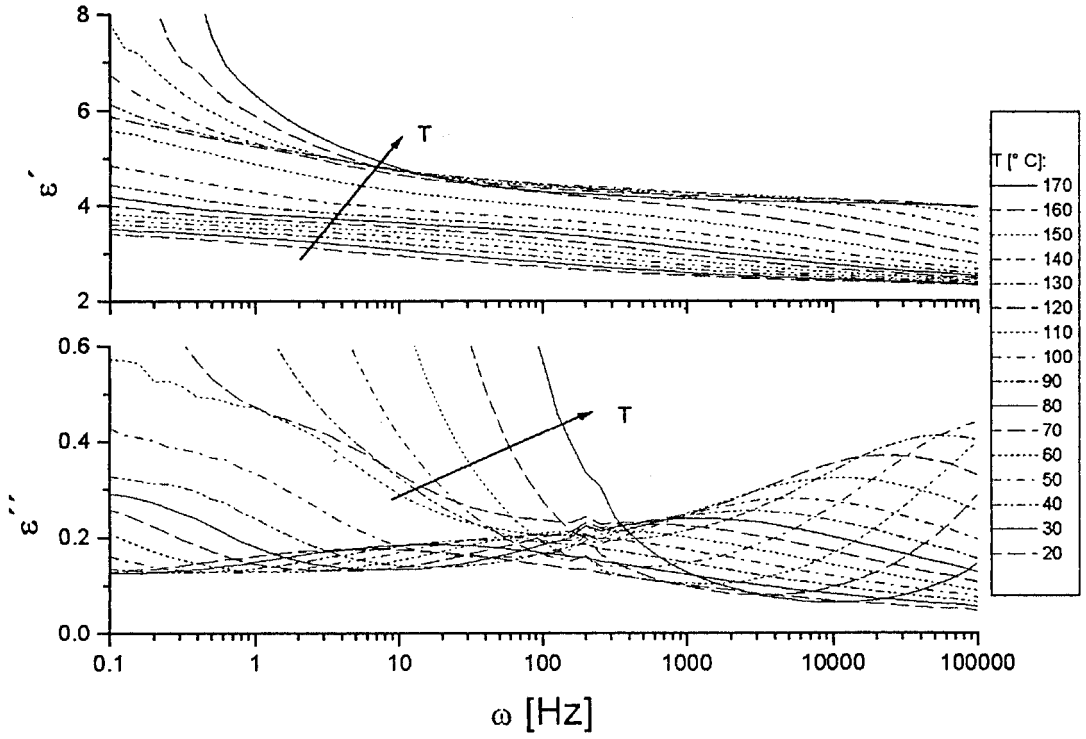

Figure 5. Frequency dependence of the dielectric function of PMMA measured by dielectric spectroscopy.

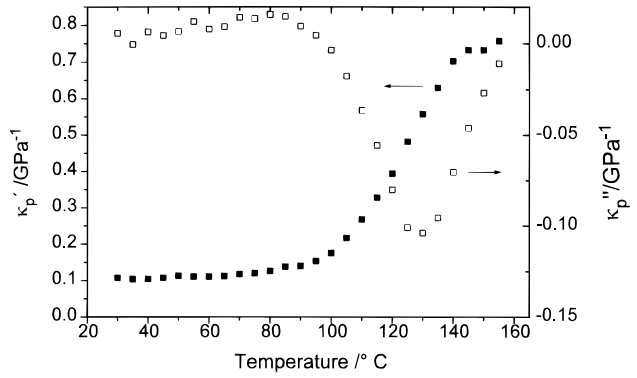

Figure 6. Temperature dependence of the real and imaginary parts of the plate compressibility κ_p of PMMA for a frequency of the sinusoidal thickness modulation of 993 Hz. The depicted values were derived from the electromechanical data shown in Figure 4 using eq 14.

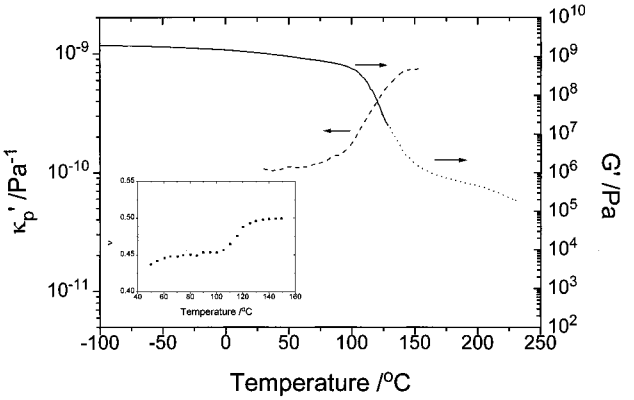

Figure 7. Temperature dependence of κ_p' and G' for PMMA. Dashed line, κ_p' determined from the electromechanical experiment for a modulation frequency of 993 Hz; solid and dotted lines, G' as shown in Figure 3 for $\omega = 100$ rad/s. Also shown is the temperature dependence of Poisson's ratio ν. Values for ν have been derived by the analysis of the electromechanical compression and the shear modulus G' using eqs 22a−c.

geometry of the electromechanical setup. This point is crucial for the exact data analysis of the electromechanical data.

At this point, it is necessary to discuss the maximum change in film thickness which can be expected due to the resistive contribution. Taking typical values for PMMA of $\alpha = 7 \times 10^{-5}$ K^{-1}, $\rho = 1.19 \times 10^3$ kg/m^3, and $c_p = 1.42 \times 10^3$ J/kg K at room temperature,[12] an applied external voltage of 100 V, a film thickness of 2.1 μm, and an imaginary part of the dielectric function $\epsilon'' = 0.5$, a change in temperature of around 8 mK, equivalent to an absolute change in thickness of 1 pm, can be expected. This value is well below the experimentally observed modulation strength. Above T_g, α increases up to about 6×10^{-4} K^{-1}, c_p increases slightly up to 10×10^3 J/kg K, and the density ρ remains almost constant.[12] Even then, Δh remains below 2 pm.

In general, also the loss parts of the elastic moduli cause a rise in sample temperature. For small oscillations, the energy ΔW_E per time and unit volume is[17]

$$\frac{\Delta W_E}{V\Delta t} \cong \frac{1}{2}\omega E''\left(\frac{\Delta h}{h}\right)^2 \tag{23}$$

Again, the amplitude of the periodic temperature modulation will depend on the driving frequency and the maximum value corresponds approximately to the energy dissipated within a half period. Since Δh is proportional to U_0^2, this contribution will oscillate at 4ω and thus not appear by lock-in detection at twice the driving frequency. A rough estimation of the resulting change in film thickness using eqs 11 and 12 and the parameters given above predicts an expansion in the femtometer range, well below the resolution of the setup. One might also presume that the applied electric field results in shear forces, causing a rotation of the film. Since the electric field induced stress is perpendicular to the sample surface, a shear force induced rotation is not possible for samples which are

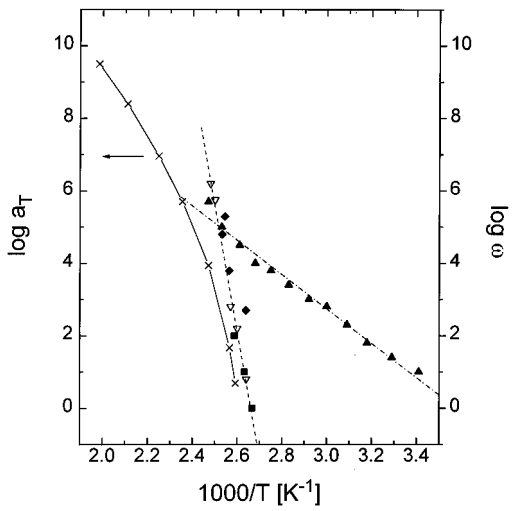

Figure 8. Comparison of relaxation times τ, expressed as log $\omega = \log(2\pi/\tau)$, determined from electromechanical experiments and mechanical and dielectric spectroscopy. Solid diamonds indicate relaxation times of the electromechanical experiments (see eq 24). Solid squares refer to the temperatures of maximum loss in the constant-frequency shear experiment (Figure 3) on 1.2 mm thick films. Solid triangles are relaxation times determined by Havriliak−Negami fits to the β-relaxation peak in the dielectric loss spectra (Figure 5). The data as indicated by open triangles are relaxation times of the dielectric α-process of PMMA.[18] Crosses refer to the temperature dependence of the shift factor a_T.

isotropic within the plane of the film. We presume that the PMMA samples analyzed in our experiments possess in-plane isotropy if averaged over the electrode area. In addition, a rotation of the electrodes can only be detected by the interferometer for the case of a very rough electrode surface.

Relaxation times have been determined from the electromechanical data in the following way. Since the out-of-phase part of the electromechanical compression is rather noisy, we have defined the relaxation temperature such that

$$\frac{\partial^2 \log|\kappa_p^{-1}|}{\partial T^2} = 0 \qquad (24)$$

For a single Debye process, this is approximately equal to the temperature of the peak maximum in the loss spectrum. The corresponding relaxation time was taken as the inverse of the modulation frequency times 2π.

Figure 8 summarizes the relaxation times as determined by mechanical and dielectric relaxation experiments in an Arrhenius-type representation:

- A master curve has been constructed from the frequency-dependent measurements of G for different temperatures. The corresponding shift factors a_T are shown as crosses.
- The temperature dependence of G was measured at 1, 10, and 100 Hz (see Figure 3). The temperatures of maximum loss G'' are indicated in Figure 8 by solid squares.
- Sasabe et al. have analyzed the dielectric properties of PMMA over 9 decades in frequency.[16] At temperatures above the glass transition temperature, the dielectric loss spectra reveal two peaks, one assigned to micro-Brownian (or segmental) motion of the main chain (α-process) and the other at higher frequency to the motion of the side chain (β-process). As stated above, the α-process in PMMA is rather weak and a decomposition of the loss spectra might be difficult. The relaxation times of the low-frequency peak are indicated by open triangles in Figure 8.
- Further shown are relaxation times of the β-relaxation process, obtained by the Havriliak−Negami analysis of the data in Figure 5.

The temperature dependence of the shift factor a_T clearly reveals non-Arrhenius behavior, which assigns this process to the α-relaxation of PMMA. Within the experimental error, the relaxation data from the thin-film electrostriction experiment, bulk modulus determination, and dielectric spectroscopy are in good agreement. The slope of the linear regressions through the experimental data points, indicated by a dashed line in Figure 8, roughly corresponds to the local tangent of the WLF curve as a function of temperature. The comparison of the apparent activation energies to that of the dielectric β-relaxation process further supports the assignment of the electromechanical relaxation to the α-process. This proves that electrostriction is a powerful method to determine the relaxation times associated with the viscoelastic properties of thin polymeric films.

Finally, we want to note that no relaxation process corresponding to the dielectric β-relaxation could be resolved in the electromechanical experiments in the frequency and temperature region studied. Further improvements in the accuracy of the setup are thus necessary.

Conclusion

The electric field induced change in film thickness of a thin organic film has been examined both theoretically and experimentally. The results show that absolute values of the elastic moduli as well as their temperature and frequency dependencies can be derived from electromechanical experiments. The periodic change in film thickness was shown to be dominated by the electrostrictional contribution, while dissipative contributions due to the imaginary parts of the dielectric function and of the mechanical moduli are only minor. The induced modulation in film thickness thus corresponds directly to an effective plate compressibility, which can be further correlated to the hydrodynamic bulk compressibility or to the Young's modulus E. An accurate determination of E however requires the knowledge of Poisson's ratio ν, which (in general) shows anisotropy and pronounced temperature and frequency dependence. If, however, E or G can be determined in a separate experiment, the combination with the electromechanical data could yield information on the time−temperature characteristics of ν.

Electromechanical experiments performed on an about 2 μm thick film of conventional PMMA as a function of frequency and temperature show a pronounced softening at the glass transition temperature. Since the frequency and temperature ranges accessible by this experiment lie within the typical window of the dielectric spectroscopy, a direct comparison of relaxation data is possible. In the case of the thin PMMA film, the temperature dependence of the electromechanical relaxation times clearly showed that the softening of the material corresponds to the dielectric α-process, supporting the assignment of the electromechanical softening to the glass transition. The analysis of the modulation amplitude of the electric field induced thickness change yielded values for the plate compressibility of 0.1 GPa^{-1} in the glassy state and of around 0.7 GPa^{-1} above T_g. These values are quite consistent with published bulk data.

Finally, we would like to point out that the method presented in this paper is applicable to films with a wide range in film thickness even down to the nanometer region, depending on parameters such as the compressibility and the dielectric breakdown field. Indeed, Langmuir−Blodgett films with thicknesses below 100 nm have been examined.[10a,19] This method thus offers the possibility to compare the mechanical moduli and dynamic behavior of films with different thicknesses, yielding information on both morphological changes and surface effects. This will be subject to further work.[19]

Acknowledgment. We thank Prof. H. H. Winter (University of Massachusetts) and Prof. G. Wegner (MPI Mainz) for support and fruitful discussions.

References and Notes

(1) Chen, Y. L.; Helm, C. A.; Israelachvili, J. N. *Langmuir* **1991**, *7*, 2694.
(2) Johannsmann, D.; Mathauer, K.; Wegner, G.; Knoll, W. *Phys. Rev. B* **1992**, *46*, 7808.
(3) Bader, S.; Kalaugher, E. M.; Arzt, E. *Thin Solid Films* **1995**, *263*, 175.
(4) Nizzoli, F.; Hillebrands, B.; Lee, S.; Stegeman, G. I.; Duda, G.; Wegner, G.; Knoll, W. *Mater. Sci. Eng.* **1990**, *B5*, 173.
(5) Han, M.-Y.; Jou, J.-H. *Thin Solid Films* **1995**, *260*, 58.
(6) Winkelhahn, H.-J.; Winter, H. H.; Neher, D. *Appl. Phys. Lett.* **1994**, *64*, 1347.
(7) Blythe, A. R. *Electrical Properties of Polymers*; Cambridge University Press: Cambridge, 1979.
(8) Jackson, J. D. *Klasische* Elektrodynamik; Walter de Gruyter: Berlin, 1983; p 184ff.
(9) Van Krevelen, D. W.; Hoftyzer, P. J. *Properties of Polymers*; Elsevier Scientific Publishers: Amsterdam, 1976.
(10) (a) Winkelhahn, H.-J., Ph.D. Thesis, Johannes-Gutenberg University, Mainz, 1995. (b) Horsthuis, W. H. G. AKZO Research Laboratories Arnheim, private communication.
(11) McCrum, N. G.; Read, B. E.; Williams, G. *Anelastic and Dielectric Effects in Polymeric Solids*; Dover Publications: New York, 1967.
(12) Brandrup, J.; Immergut, E. H., Eds. *Polymer Handbook*; John Wiley & Sons: New York, 1975; p V-55ff.
(13) Schenkel, G. *Kunststoffe* **1973**, *63*, 49.
(14) Koppelmann, J. *Rheol. Acta* **1958**, *1*, 20.
(15) Yee, A. F.; Takemori, M. T. *J. Polym. Sci., Polym. Phys. Ed.* **1982**, *20*, 205.
(16) Gilmour, I. W.; Trainor, A.; Haward, R. N. *J. Appl. Polym. Sci.* **1979**, *23*, 3129.
(17) Ferry, J. D. *Viscoelastic Properties of Polymers*; John Wiley & Sons: New York, 1980.
(18) Sasabe, H.; Saito, S. *J. Polym. Sci., Part A-2* **1968**, *6*, 1419.
(19) Jaworek, Th.; Glasser, G.; Neher, D., to be submitted.

MA960080K